

# Prediction of Creep Behavior for Cohesive Soils

## 점성토에 있어서의 크리프 거동 예측

Kim, Dae-Kyu<sup>1</sup>

김 대 규

### 요 지

본 연구에서는 탄.소.점성 구성모델을 비교적 간단한 수학적 합성유도방식에 기초하여 제안하였다. 이를 위하여 비등방성 modified Cam-Clay model을 일반응력공간으로 확장시켰으며 generalized viscous theory를 단순화하여 각각 소성 및 점성의 구성관계로 활용하였다. Damage 원리를 구성모델에 추가하였으며, 모든 식의 변형 및 개발은 모델정수의 수를 감소시키는 원칙에 입각하여 수행하였다. 개발된 구성모델을 활용하여 점성토의 크리프 거동을 예측하였으며 이를 실험결과와 비교분석하였다. 예측된 결과는 크리프파괴의 경우를 포함한 실험결과와 비교적 양호하게 일치하는 결과를 보여주었다.

### Abstract

An elastic-plastic-viscous constitutive model was proposed based on a simple formulation scheme. The anisotropic modified Cam-Clay model was extended for the general stress space for the plastic simulation. The generalized viscous theory was simplified and used for the viscous constitutive part. A damage law was incorporated into the proposed constitutive model. The mathematical formulation and development of the model were performed from the point of view that fewer parameters be better employed. The creep behaviors with or without creep rupture were predicted using the developed model for cohesive soils. The model predictions were favorably compared with the experimental results including the undrained creep rupture, which is an important observed phenomenon for cohesive soils. Despite the simplicity of the constitutive model, it performs well as long as the time to failure ratio of the creep rupture tests is within the same order of magnitude.

**Keywords :** Damage, Generalized viscous theory, Modified Cam-Clay, Rupture, Undrained creep

## 1. Introduction

Time-dependent behavior has been established as an important phenomenon for cohesive soils. Creep, strain rate effect, and thixotropy are such behaviors as considered essential in soil mechanics. The time-dependent behavior is mainly due to the low permeability and the very small plate-like particles of cohesive soils. Creep might be the most important time-dependent pheno-

menon. The primary consolidation and the secondary compression have been respectively regarded as drained and undrained creeps. Especially, the rapid large creep strain in undrained creep test may occur after the steady stage with relatively small creep strain. This is called the undrained creep rupture and it significantly affects the overall stability and should be considered in geotechnical analysis.

The appropriate simulation of the creep behavior has

<sup>1</sup> Member, Assistant Prof., Dept. of Civil and Environ. Engrg. Sang-Myung Univ. (daekyu@smu.ac.kr)

been studied through the mathematical and physical modeling (Aubry et al., 1985; Chiarelli et al., 2003). Most of them have adopted a viscous theory and regarded soils in macroscopic view, in other words, soils were assumed very homogeneous throughout the entire soil mass; however, soils, in practice, can be damaged in patches during deformation. In that sense, a few efforts to properly describe the creep behavior have been made especially in attempting to incorporate the damage into the constitutive models (Singh and Mitchell, 1968; Aubry et al., 1985; Vyalov, 1986; de Sciarra, 1997; Jenson et al., 2001; Chiarelli et al., 2003).

In this research, a combined elastic-plastic-viscous constitutive relation has been developed. The generalized Hooke's law was used for the elastic part. The anisotropic modified Cam-Clay model (Dafalias, 1987) was extended for the general stress space and used for the plastic part in this research. The anisotropic modified Cam-Clay model proposed is directly based on the isotropic modified Cam-Clay model that employs the solid critical state theory, and the model has given good predictions with few model parameters. The generalized viscous theory by Perzyna (1966) has the advantages that it has successfully simulated the time-dependent behavior of soils with few model parameters, and the mathematical form of the theory can be easily formulated with the classical elastic-plastic derivation. The generalized viscous theory was simplified, in this research, for effective viscous modeling and obvious mathematical formulation in an elastic-plastic-viscous combination scheme. A damage law has been incorporated into the constitutive relation based on Vyalov (1986). The physical and mathematical formulation of the combined model was performed from the point of view that fewer parameters be better employed. The model predictions have been compared with the experimental results of creep tests. The concepts of the constitutive models, the damage law, the theoretical and mathematical formulation, and the comparison and investigation of the results are described in following sections.

## 2. Concepts and Applications of Models

### 2.1 Simplification of Generalized Viscous Theory

The concept and the simplification, made in this research, of the generalized viscous theory (Perzyna, 1966) are briefly described in this section. The basic assumption of the theory is that the total strain rate can be resolved into time-independent elastic and plastic, and time-dependent plastic parts, which is called viscoplastic strain rate. The viscoplastic strain rate tensor  $\dot{\epsilon}_{ij}^{vp}$  is given by:

$$\dot{\epsilon}_{ij}^{vp} = \langle \Phi(F) \rangle \frac{\partial f}{\partial \sigma_{ij}} \quad (1)$$

where  $\langle \rangle$  is Macauley bracket and  $F$  represents the initial yield function, and is also called "the static yield function". The viscoplastic strain rate tensor assumes a function of the "excess stress" or "overstress" located on the initial yield locus. The  $f$  defines so called "dynamic loading surface". The magnitude of the viscoplastic strain rate is controlled by the value of the viscous or overstress flow function  $\langle \Phi(F) \rangle$ .

A common assumption of the classical inviscid plasticity and the generalized viscous theory is the decomposition of strain into elastic and inelastic deformations; however, a fundamental difference exists in that the stress point must be on or within the yield surface in the inviscid plasticity theory, on the other hand, in the generalized viscous theory, the stress point can be outside the initial yield surface, instead, the dynamic loading surface passes through the loading point (Fig. 1). On this surface, the viscoplastic strain rate is not zero, and its magnitude depends on the overstress flow function  $\Phi(F)$ . In inviscid plasticity, plastic strain is obtained from a consistency condition applied to the yield function. In the generalized viscous theory, it is assumed that the viscoplastic strain is a function of an overstress on the initial yield function, i.e., the magnitude of the viscoplastic strain rate depends on the overstress flow function. Its direction is given by the gradient vector  $\partial f / \partial \sigma_{ij}$ , and as in the associated flow rule of inviscid plasticity, is in

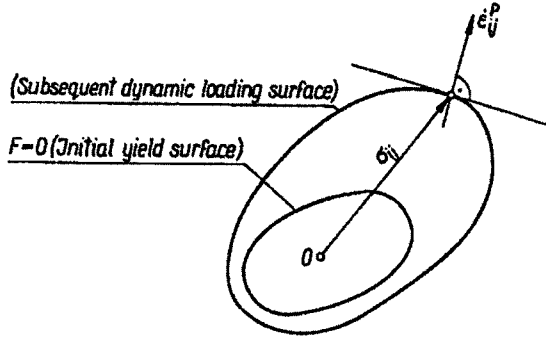


Fig. 1. Yield surfaces and strain rate vector (Perzyna, 1966)

the outward normal direction of the dynamic loading surface. The functional form of the overstress flow function is selected based on experimental results. Two forms in Eq. (2) are commonly used, where  $n$  is a model parameter. The initial yield surface evolves exactly as in plasticity and serves only to separate the region of stress space where deformation is both elastic and viscoplastic from the region where only elastic deformation takes place and viscoplastic deformation is zero. The dynamic loading surface evolves similarly to the initial yield surface but it is also dependent on the rate of loading in addition to stress and strain.

$$\Phi(F) = F^n \quad \text{or} \quad \Phi(F) = \exp F - 1 \quad (2)$$

In this research, the generalized viscous theory stated above is simplified as: the initial yield surface and the dynamic loading surface are not differentiated so only one loading surface exists to separate only elastic deformation at the stress state inside the surface from both elastic and viscoplastic deformation at the stress state on the surface. This is the same as in inviscid plasticity. The further assumptions are that the loading surface has the exactly same functional form and hardening rules with the plastic loading function. The right side of Eq. (2), with no model parameter, was used as the overstress flow function since this research mainly focuses on the damage effect rather than time-dependent or viscous model itself.

## 2.2 Extension of Anisotropic Modified Cam-Clay Model

Dafalias (1987) developed an anisotropic version of the modified Cam-Clay model, by incorporating an anisotropic hardening parameter  $\alpha$  into the yield function  $f$  as in Eq. (3), for the triaxial stress condition.

$$f = p_2 - p p_0 + \frac{1}{M} (q_2 - 2\alpha p q + \alpha^2 p p_0) = 0 \quad (3)$$

where  $p$  and  $q$  respectively denote the mean effective stress and the deviatoric stress;  $M$  is the slope of the critical state line;  $p_0$  is the apex of the yield surface;  $\alpha$  is the anisotropic hardening parameter and its evolution is given as Eq. (4).

$$\dot{\alpha} = \langle \bar{\lambda} \rangle \left\{ \frac{1 + e_0}{\lambda - \kappa} \left| \frac{\partial f}{\partial p} \right| \frac{c}{p_0} (q - x \alpha p) \right\} \quad (4)$$

where  $\langle \rangle$  = Macauley bracket;  $\bar{\lambda}$  = loading index;  $\lambda$  = compression index from the  $e$  versus  $\ln p$  curve;  $\kappa$  = recompression index from the  $e$  versus  $\ln p$  curve;  $e_0$  = initial void ratio;  $c$  and  $x$  = constants. The expression  $\langle \bar{\lambda} (\partial f / \partial p) \rangle$  represents the plastic strain rate  $\dot{\epsilon}^p$ .

To extend eqs. (3) and (4) from the triaxial stress space to the general stress space, minor changes are made, in this research, for  $q$  and  $\alpha$ , such as  $q = \{(3/2) s_{ij} s_{ij}\}^{1/2}$  and  $\alpha = \{(3/2) \alpha_{ij} \alpha_{ij}\}^{1/2}$ . Eqs. (3) and (4) are now generalized as follows:

$$f = p^2 - p p_0 + \frac{1}{2M^2} \{ (s_{ij} - \alpha p_{ij})(s_{ij} - \alpha p_{ij}) + (p_0 - p) p \alpha_{ij} \alpha_{ij} \} = 0 \quad (5)$$

$$\dot{\alpha} = \langle \bar{\lambda} \rangle \left\{ \frac{1 + e_0}{\lambda - \kappa} \left| \text{tr} \frac{\partial f}{\partial \sigma_{mn}} \right| \frac{c}{p_0} (s_{ij} - x p \alpha_{ij}) \right\} \quad (6)$$

The modified Cam-Clay model might be one of the most popular constitutive models for cohesive soils since it is based on the relatively simple but solid theory, and can well predict the plastic behavior with only a few model parameters. In the modified Cam-Clay model,  $p_0$  always locates on the  $p$  axis with no rotation of the yield surface, and serves as a hardening parameter. The critical

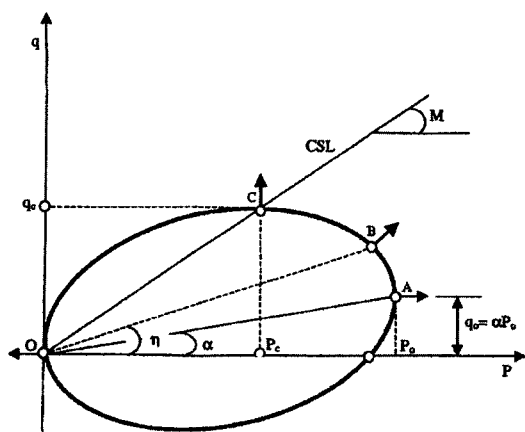


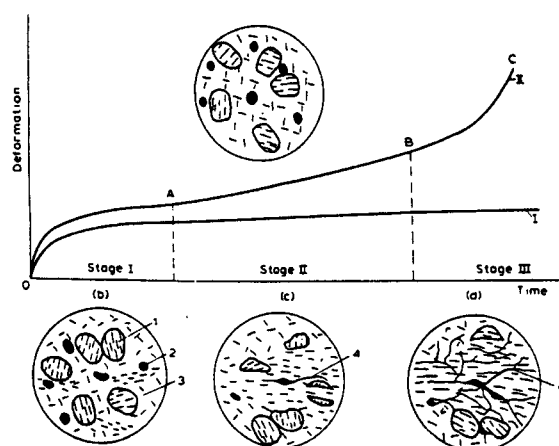
Fig. 2. Anisotropic modified Cam-Clay model (Dafalias, 1987)

strate line should meet the yield locus at  $p_c/2$ . It should be noted that the modified Cam-Clay model was proposed basically for the normally and isotropically consolidated cohesive soils and accordingly isotropic hardening rule was adopted. In the anisotropic modified Cam-Clay model, when the yield locus in the principal stress space undergoes kinematic hardening, the yield locus will move around the  $\pi$ -plane. This behavior will appear as the rotation of the yield locus in the principal stress space. In  $p$  versus  $q$  plane, the shape of the yield locus is the inclined cut of the 3D yield locus that appears in Fig. 2. Thus kinematic hardening will result in the rotation of the elliptical yield locus in  $p$ - $q$  space for which the origin does not change. Consequently, the shape of the yield locus will be a distorted ellipse when subjected to anisotropic hardening.

### 2.3 Damage Model

Vyalov (1986) presented Fig. 3 as a general hypothesis quantitatively describing the complete creep process of cohesive soils under a sustained load. The creep curve has usually three stages: (stage I) primary creep where the strain rate gradually decreases with time. (stage II) steady state or secondary creep with constant rate, leading to a period of linear strain versus time response. (stage III) tertiary creep where creep rate begins to rapidly increase.

Each particle, as in Fig. 3, is linked at the neighboring particles by at least two bonds. When there is only one



1=micro-aggregates of particles, 2=cavities and voids  
3=cementing clay, 4=micro and macro-cracks

Fig. 3. Creep mechanism (Vyalov, 1986)

bond due to Van der Waals' forces and so on, the soil structure is considered disturbed. Any point of disturbance of the bonding is termed "defect". Voids containing free water are not considered defects. In stiff clay soils, defects manifest themselves in the form of micro-cavities, voids, microcracks, or cleavage, etc. These defects in soil structure are considered the prime factors causing creep rupture. During the primary creep stage, microcracks tend to close, and cavities and voids contract and expand in the direction of shear. This leads to compaction of the soil and the formation of new interparticle bonds. As a result, the deformation attenuates in time. During the secondary creep stage, more microcracks begin to propagate, and more particles are oriented with their basal surfaces in the direction of shear. Therefore, there is a continuous "healing" of the defects but also a fresh disturbance in the form of microcracks is formed. Finally, as deformation progresses, and following the onset of the tertiary creep stage, an intensive propagation of microcracks takes place. Eventually, these microcracks form larger cracks, causing failure of the specimen. Based on microscopic observation as stated above, it has been concluded that there are two phenomena responsible for soil creep, i.e., the hardening and the softening of soil. If hardening is dominant, the deformation attenuates in time, and the creep curve response possesses only the primary and secondary stages. If, on the other hand,

softening prevails, the creep rate will accelerate and the tertiary stage of creep may terminate in rupture.

Kachanov (1967) suggested that this increase in strain rate be described by the introduction of an additional variable into the constitutive equation. This additional variable, termed  $\omega$ , is considered to be a measure of "damage" incurred by the material under sustained loading. As time passes, damage accumulates, and the value of  $\omega$  evolves according to a certain rate equation.

This concept of damage has been widely used in modeling the strength deterioration of metals, which is due in part to its simplicity. Aubry et al. (1985) have also adopted this concept in some studies pertaining to clay behavior. In this research, the same approach was adopted, where soil damage is represented by the single damage variable  $\omega$ . During the tertiary creep stage, structural defects develop at a drastic rate and, once the structural damage  $\omega$ , reaches a critical value  $\omega_f$ , the soil is considered to have creep failed.

### 3. Mathematical Formulation of the Models

In this section, the combination and mathematical formulation of elastic, plastic, and viscous constitutive equations is described. The basic concept is as Eq. (7) and it is based on Dafalias (1982). The revision and application of each model, made in this research, were performed so that each model may employ fewer parameters for the practically easy usage of the model and for the avoidance of the confusion with the complicated parameters. The superscripts  $e$ ,  $p$ ,  $vp$  denote elastic, time-independent plastic, and time-dependent viscoplastic parts, respectively. The time-dependent behavior is assumed to be attributed to only the coupling of plastic and viscous parts, i.e., viscoplastic part.

$$\dot{\epsilon}_{ij} = \dot{\epsilon}_{ij}^e + \dot{\epsilon}_{ij}^p + \dot{\epsilon}_{ij}^{vp} \quad (7)$$

The elastic strain rate is time-independent and obtained using the generalized Hooke's law. The time-independent plastic strain rate is represented by the associated flow rule of Eq. (8), where the anisotropic modified Cam-Clay

loading function, Eq. (5), is used as the loading function  $f$ .

$$\epsilon_{ij}^p = \langle L \rangle \frac{\partial f}{\partial \sigma_{ij}} \quad (8)$$

The time-dependent viscoplastic strain rate is estimated using Eq. (1). In this research, as stated in section 2.1, only one loading surface is assumed to separate elastic deformation at the stress state inside the surface from both elastic and viscoplastic deformation at the stress state on the surface. Regarding the viscoplastic behavior, the loading surface is assumed to have the same functional form and hardening rules with the plastic loading function in Eq. (5). The right side of Eq. (2) is used as the overstress flow function.

In this research, soil damage is represented by the single damage variable  $\omega$ , as stated in section 2.3, in the form of Eq. (9) based on Vyalov (1986).

$$\omega = 1 - \frac{(1 - \omega_o)}{(1 + t)^{\Lambda \bar{\tau}}} \quad 1 - \omega = (1 - \omega_o) (1 + t)^{-\Lambda \bar{\tau}} \quad (9)$$

where  $\omega$  is the degree of damage at any time  $t$ ,  $\omega_o$  is the initial structural damage,  $\Lambda$  is constant, and  $\bar{\tau}$  is a dimensionless stress function representing the magnitude of an applied deviatoric stress.  $t$  is a dimensionless quantity equal to the value of period of deformation  $t$  divided by  $t^m$ , where  $t^m$  is a parameter measured in units of time, and may be taken to be equal to one. The quantities  $1 - \omega_o$  and  $1 - \omega$  define the undamaged areas of soil at the initial condition and at any time  $t$ , respectively. If  $\omega_f$  is used, it indicates the degree of damage at the moment of failure ( $t=t_f$ ).

According to a proper assumption of  $\bar{\tau}$  based on Regel et al. (1974) and Vyalov (1986), Eq. (9) yields:

$$\omega = 1 - \frac{(1 - \omega_o)}{(1 + t)^{\frac{\Lambda \tau_o}{\tau_o - \tau}}} \quad (10)$$

where  $\tau_o$  is the hypothetical instantaneous strength of the soil and the value should be determined from the creep test; however,  $\tau_o$  is assumed to be undrained shear strength so that the value of which can be practically

determined from the time-independent triaxial test.  $\tau$  is the applied deviatoric stress. Eq. (10) defines the damage incurred by the soil at any time  $t$  and for any given applied load  $\tau$ . It is obvious that the higher the hypothetical instantaneous strength of the soil  $\tau_o$ , the smaller the changes in  $\omega$ . Also, as expected, the degree of structural damage increases as the applied stress increases. The significance of Eq. (10) rises from the fact that all parameters except  $\Lambda$  have a quite definite physical meaning. The initial degree of damage  $\omega_o$  and the constant  $\Lambda$  can be evaluated through microscopic investigation of a soil sample. Due to the difficulty in determining the microscopic data, it is often and successfully assumed that the values of  $\omega_o$  and  $\Lambda$  are obtained from conventional creep test. This represents that the constants  $\tau_o$ ,  $\omega_o$ , and  $\Lambda$  were included originally for predicting the change of the structural damage  $\omega$ . Here, the essence of these constants changed from those of microscopically-based parameters to macroscopic parameters. If it is further assumed that soil is initially not damaged, then  $\omega_o=0$ , and Eq. (10) becomes

$$\omega = 1 - \frac{1}{(1+t)^{\frac{\Lambda\tau}{\tau_o - \tau}}} \quad (11)$$

Eq. (11) indicates the degree of structural damage  $\omega$  under any applied load  $\tau$  and at any elapsed time  $t$ . One approach for incorporating the damage law into the proposed model is based on the concept of net stress. The quantity  $1-\omega$  represents the intact area of a unit cross-section. The damage accumulates and the amount of material available for carrying the applied load is reduced, thus net stress increases. Based on this proposition, the stress is given by Eq. (12) (Al-Shamrani and Sture, 1994).

$$\sigma_{ij} = \frac{\sigma_{ij}}{1-\omega} \quad (12)$$

Eqs. (11) and (12) were adopted in this research as they have physical meanings and have been accepted for various kinds of material.

#### 4. Prediction Results and Discussions

Soils may fail under a sustained load, depending on the mechanical characteristics, the magnitude of the applied load, and the stress history but the physical mechanism that causes undrained creep rupture in cohesive soils is not yet fully understood. In this section, the validity of the developed model in simulating some available creep test results, including creep rupture, is examined. Three experimental programs carried out for Bay mud (Bonaparte, 1981; Borja, 1984), Osaka clay (Murayama et al., 1970; Sekiguchi, 1984), and Haney clay (Vaid and Campanella, 1977; Matsui and Abe, 1988) have investigated the undrained creep behavior of normally consolidated cohesive soils.

The creep behavior of anisotropically consolidated soils has been rarely studied. Bonaparte (1981) and Borja (1984) conducted a series of anisotropic triaxial undrained creep tests on undisturbed San Francisco Bay mud. The soil specimens were first consolidated isotropically to a confining pressure of  $0.3 \text{ kg/cm}^2$ . Then the axial load was increased in small increments until the stress ratio was equal to 2.0. Thereafter, the specimens were anisotropically consolidated by simultaneously increasing the axial load and the cell pressure so that the stress ratio was maintained at 2.0 throughout the consolidation. The load increments were applied at approximately 8 hour interval, and each increment was less than 10% of the undrained shear strength. Once the proper consolidation stress was reached, a prescribed deviatoric stresses ( $0.53, 0.55, 0.57, 0.60 \text{ kg/cm}^2$ ) were applied and the creep tests initiated.

The observed and predicted creep curves for the four creep tests are shown in Figs. 4 and 5. The set of the input parameters are listed in Table 1. The values of the input parameters were evaluated using the test results by Bonaparte (1981) and Borja (1984). The hypothetical instantaneous strength parameter  $\tau_o$  was assumed to be equal to the undrained shear strength ( $1.4 \text{ kg/cm}^2$ ) obtained from the test results. It was reported that the two creep tests with deviatoric stress equal to  $0.57$  and  $0.60 \text{ kg/cm}^2$  clearly resulting in creep rupture eventhough it is true that the other two tests are likely to fail in

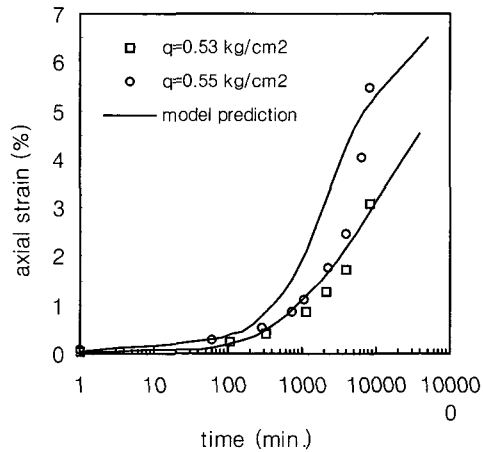


Fig. 4. Creep behavior (Bay mud, deviatoric stress 0.53, 0.55 kg/cm<sup>2</sup>)

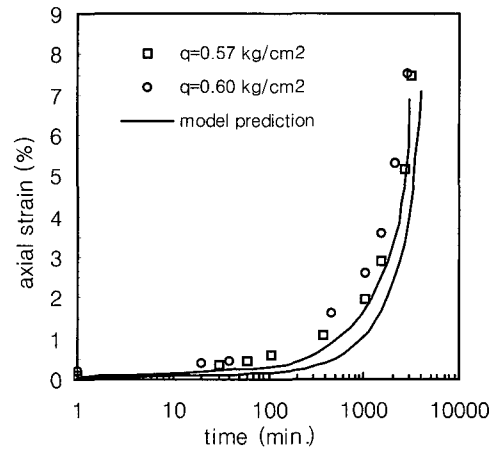


Fig. 5. Creep behavior (Bay mud, deviatoric stress 0.57, 0.60 kg/cm<sup>2</sup>)

Table 1. Input parameters (Bay mud)

parameter	identification	value
$M$	slope of CSL	1.40
$\lambda$	slope of NCL	0.37
$\kappa$	slope of swelling line	0.054
$\nu$	poisson's ratio	0.3
$e_o$	initial void ratio	2.52
$c$	anisotropic hardening parameter	0.2
$x$		0.1
$\tau_o$	damage parameter	1.4kg/cm <sup>2</sup>
$\Lambda$		$1.5 \times 10^{-4}$

rupture. The damage parameter  $\Lambda$  was determined by matching the results of these two creep rupture tests.

From Figs. 4 and 5, it can be noted that agreement between the experimental and predicted behavior is acceptable, considering the relatively simple constitutive model. For the other two tests in Fig. 5, where creep rupture clearly took place, the model predictions underestimate the experimental creep strain. It was possible, though, to use a larger value for the damage parameter  $\Lambda$ , which would have improved the prediction. However, that leads to an overestimation of the final values of the creep strain. For this reason,  $\Lambda$  was set equal to zero in predicting the results of the creep tests with deviatoric stresses equal to 0.53 and 0.55 kg/cm<sup>2</sup>. Otherwise, the model prediction of these tests would end in rapid creep rupture. Another more realistic alternative approach for the creep behavior with rupture is to assume that the

initial damage  $\omega_o$  is not zero as for Osaka clay stated below. In this case, two different values of  $\omega_o$  can be used for the creep tests with rupture, on the other hand, a fixed value for  $\Lambda$  is used for all of the tests with and without rupture. For the case of Bay mud, the first approach using a relatively small value of  $\Lambda$  was adopted instead of the second approach using the initial damage  $\omega_o$  since the two methods were expected to be compared with each other through the cases of Bay mud and Osaka clay.

It is important to point out that it might have been possible to use the isotropic modified Cam-Clay model instead of its anisotropic version used in this research. The prediction would not have been as good as it appears in Figs. 4 and 5. The parameters  $c$  and  $x$  differentiate the isotropic application from the anisotropic application of the modified Cam-Clay model in section 2.2. The values of  $c$  and  $x$  were determined by best-fit of the conventional triaxial test results in Bonaparte (1981) and Borja (1984).

The identification and the determination of the model parameter are practically most important in the usage of a constitutive model. In the sense, the relatively simple and basic form of the time-dependent constitutive relation, described in section 2.1, was developed and used in this research since the complexity due to the model parameters was not preferred in the mathematical viscous formulation and determining values. The constitutive model could give better predictions if more precise

but complicated viscous model was used. Regarding the viscous constitutive modeling, the respective consideration of the initial yield surface and the dynamic loading surface might be another development. The contribution of the anisotropic modified Cam-Clay model could be appreciated in that the normally consolidated specimen, on which the model is principally based, was used for the test and the prediction.

It is undesirable that the value of parameter  $\lambda$ , in this research, was determined from the best match of the test whose result was predicted using the parameter value, eventhough the parameter value was used to simulate the results of the other tests; however, this is proper for the case that the specimen from a construction site is tested, then the parameter values determined from the test results are used to predict the soil behavior due to the actual construction.

Murayama et al. (1970) conducted a series of undrained creep tests for undisturbed normally consolidated clay from Osaka. The index properties of the clay are referred to in Sekiguchi (1984). In carrying out the test program, the specimens were consolidated to a vertical pressure, equal to  $3.0 \text{ kg/cm}^2$  for 24 hours. Then a prescribed deviatoric stress was applied to each specimen in a single increment. The applied deviatoric stresses were 1.20, 1.80, 1.99, 2.19, and  $2.30 \text{ kg/cm}^2$ .

Figs. 6 to 8 show the experimental results and the model predictions under the deviatoric stresses. The creep strains for two of these tests attenuated after some time had elapsed (Fig. 6), while in the other tests (Figs. 7 and 8), creep rupture took place, with time to failure ranging from 400 to 18000 minutes, depending on the value of the applied deviatoric stress.

Values for the input parameters used in predicting the experimental results are shown in Table 2. The input parameter values  $M$ ,  $\lambda$ ,  $\kappa$ ,  $\nu$ ,  $e_o$ ,  $c$ ,  $x$  were taken from Sekiguchi (1984) and Murayama et al. (1970) that represented the results of the conventional triaxial and oedometer tests as well as the creep tests. Specially, parameter  $c$  assumed zero to resolve the plastic yield function Eq. (5) to that of the anisotropic modified Cam-Clay model regardless of the parameter  $x$ . The

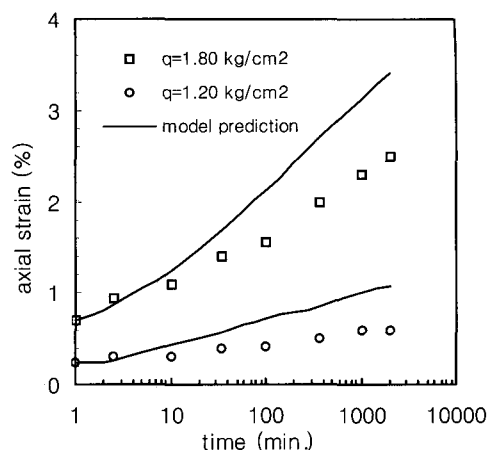


Fig. 6. Creep behavior (Osaka Clay, deviatoric stress 1.20, 1.80  $\text{kg/cm}^2$ )

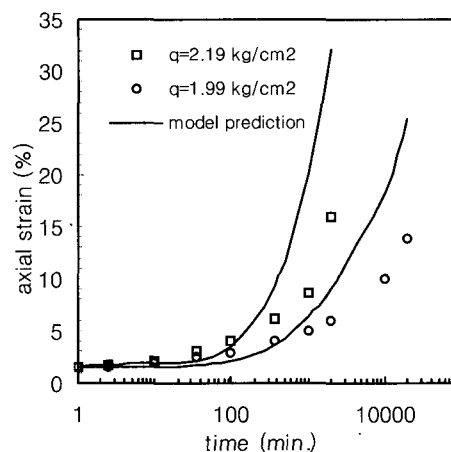


Fig. 7. Creep Behavior (Osaka Clay, deviatoric stress 1.99, 2.19  $\text{kg/cm}^2$ )

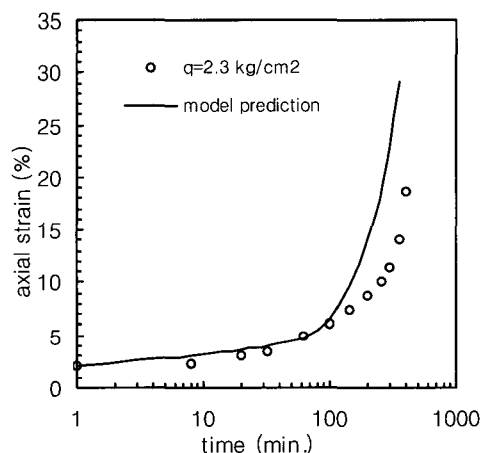


Fig. 8. Creep behavior (Osaka Clay, deviatoric stress 2.30  $\text{kg/cm}^2$ )

damage parameter  $\lambda$  was determined by simulating the results of tests that have failed in creep rupture. The instantaneous strength parameter  $\tau_o$  was taken to be



Table 2. Input parameters (Osaka clay)

parameter	identification	value
$M$	slope of CSL	1.47
$\lambda$	slope of NCL	0.343
$\kappa$	slope of swelling line	0.105
$\nu$	poisson's ratio	0.3
$e_o$	initial void ratio	1.31
$c$	anisotropic hardening parameter	0
$x$		0.1
$\tau_o$	damage parameter	3.0kg/cm <sup>2</sup>
$\Lambda$		$1.2 \times 10^{-6}$

equal to the undrained shear strength for the tested clay.

Considering the simplicity of the constitutive model, the model predictions, as noted in Figs. 6 to 8, are generally in good agreement with the experimental results. It could be noted that the inclusion of the damage law produced good prediction for the creep rupture cases with the creep stresses equal to 1.99 and 2.19 kg/cm<sup>2</sup>; however, as the applied deviatoric stress becomes larger than 2.19 kg/cm<sup>2</sup> (Fig. 8), namely over 73% of the undrained shear strength  $\tau_o$ , it had not been possible to obtain a good simulation of creep tests using the same value of the damage parameter in Table 2. It is necessary to use larger value for the damage parameter  $\Lambda$  to acquire better prediction. Instead, it might be more realistic to think that, for those specimens which failed in a relatively short time, they have incurred damage before creep tests began. This is obvious if we notice, for example, that as the applied load increases, just from 1.99 to 2.30 kg/cm<sup>2</sup>, the time to failure reduced from 18,000 to 400 minutes. In other words, 15.5% increase in the applied load led to about a 98% reduction in the time to failure. Thus a more likely possibility is that the damage was actually substantiated during the application of the deviatoric stress, and not after the initiation of the creep test. If this proposition is true, then instead of considering the soil to be undamaged before creep test starts, and the initial damage parameter  $\omega_o$  should assume a none-zero value. The prediction of the creep test under 2.30 kg/cm<sup>2</sup> stress level is presented in Fig. 8. The initial damage parameter  $\omega_o$  was assigned a value of 0.0015, while the values of the other parameters are the same as those in Table 2. As would be expected, the

inclusion of the initial damage led to an overestimation of creep strain for the initial part of the creep curve instead of producing relatively better simulation near creep rupture.

Vaid and Campanella (1977) and Matsui and Abe (1988) carried out a number of undrained creep tests for undisturbed Haney clay in America. Prior to the application of the prescribed deviatoric stress, the specimens were isotropically consolidated to a confining pressure equal to 5.25 kg/cm<sup>2</sup> for 36 hours. Principal stress difference, i.e., deviatoric stress was applied in one increment. The set of input parameters used in simulating the creep tests for Haney clay is listed in Table 3. The parameter values of  $M$ ,  $\lambda$ ,  $\kappa$ ,  $\nu$ ,  $e_o$ ,  $c$ ,  $x$  were taken from the conventional triaxial and oedometer test results of Vaid and Campanella (1977) and Matsui and Abe (1988). The parameter  $c$  assumed zero, as in Osaka clay, to reduce the plastic yield function Eq. (5) to that of the anisotropic modified Cam-Clay model. In this case, the parameter  $x$  has no influence on the constitutive relation so 0.1 was simply assumed as the value of  $x$ . The value of the damage parameter  $\Lambda$  was determined by matching the results of creep tests that have failed. The instantaneous strength parameter  $\tau_o$  was taken to be equal to the undrained shear strength 3.5 kg/cm<sup>2</sup> from time-independent undrained triaxial test.

Figs. 9 through 11 show the experimental and predicted creep curves for five creep tests of Haney clay. It is noted that the three tests, under stress levels of 1.96, 2.34 and 2.63 kg/cm<sup>2</sup>, did not experience creep rupture, rather, creep attenuated with time. On the other hand, for stress levels of 2.72 and 2.78 kg/cm<sup>2</sup>, the specimens have

Table 3. Input parameters (Haney clay)

parameter	identification	value
$M$	slope of CSL	1.29
$\lambda$	slope of NCL	0.20
$\kappa$	slope of swelling line	0.031
$\nu$	poisson's ratio	0.3
$e_o$	initial void ratio	1.896
$c$	anisotropic hardening parameter	0
$x$		0.1
$\tau_o$	damage parameter	3.5kg/cm <sup>2</sup>
$\Lambda$		$1 \times 10^{-6}$

failed. It was necessary for the simulation of the creep rupture test, under deviatoric stress of  $2.78 \text{ kg/cm}^2$ , to use a value of  $0.0004$  for the initial damage  $\omega_o$ .

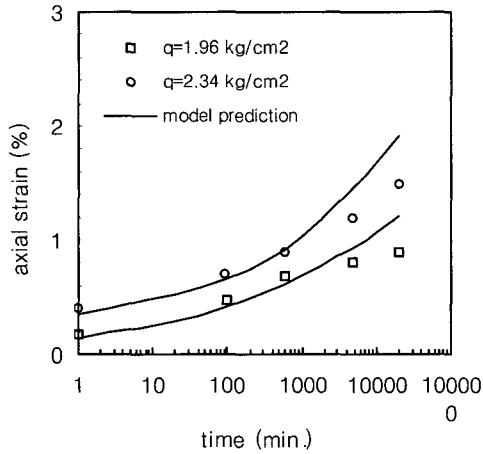


Fig. 9. Creep behavior (Haney clay, deviatoric stress 1.96, 2.34  $\text{kg/cm}^2$ )

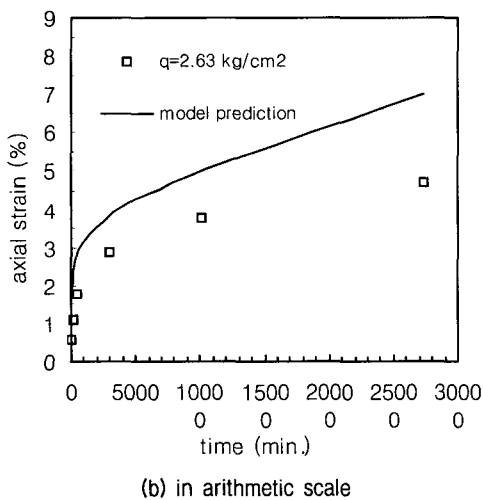
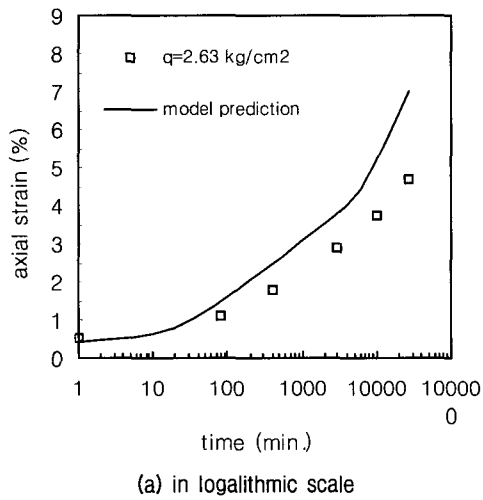


Fig. 10. Creep behavior (Haney clay, deviatoric stress 2.63  $\text{kg/cm}^2$ )

Although it may seem, from Fig. 10 (a), that the creep test with the applied stress of  $2.63 \text{ kg/cm}^2$  has the potential to fail, as can be noted from Fig. 10 (b) where time and axial strain are both plotted in arithmetic scales, tertiary creep stage has not started. This, however, does not rule out the possibility that the creep strain will start to accelerate after some time. On the contrary, this represents how long a creep test should last before it can finally be determined whether creep will attenuate with time or accelerate to rupture.

It is clear that the introduction of initial damage makes it possible to simulate the results of creep rupture tests under high stress level, using the same damage parameters for all the tests. This, however, works well as long as the time to failure for different tests is within the same order of magnitude. If the difference in time to rupture among the creep rupture tests is large, then different values for the initial damage  $\omega_o$  must be used for different tests. Admittedly, this is the main limitation of the present damage law.

It can be observed that the overall creep response depends on the level of applied load. If the load is low, hardening will prevail, and creep deformation will attenuate. For moderately high loads, the phenomenon of soil hardening occurs at the stage of primary creep and the soil softens. However, after a certain period of elapsed time, the softening is compensated for by a hardening, and the creep reaches a stage of steady state wherein the rate is approximately constant. Finally, when

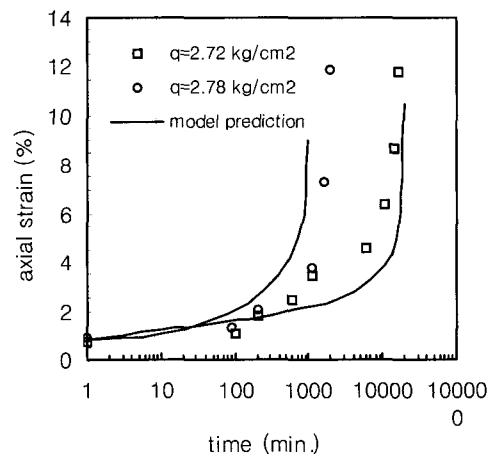


Fig. 11. Creep behavior (Haney clay, deviatoric stress 2.72, 2.78  $\text{kg/cm}^2$ )

the applied load is high, the structural damage accumulated during the course of deformation will be large, which then leads to a prevalence of softening as opposed to hardening. Consequently, the deformation rate increases, marking the offset of the tertiary creep stage.

## 5. Conclusions

A combined elastic-plastic-viscous constitutive model was developed based on a simple formulation scheme. The generalized Hooke's law was used as the elastic part. The anisotropic modified Cam Clay model by Dafalias (1987) was extended for the general stress space and used for the plastic part. The generalized viscous theory by Perzyna (1966) was simplified and used for the viscous constitutive part. A damage law proposed by Vylov (1986) was incorporated into the developed constitutive model. The mathematical formulation and development of the model was performed from the point of view that fewer parameters be better employed. The creep behavior with or without creep rupture was predicted using the developed model for cohesive soils. Comparing the model prediction and the experimental result for the Osaka clay, the Bay mud, and the Haney clay, the following conclusions can be made.

- (1) The prediction conducted using the proposed constitutive model generally agreed well with the experimental creep strain of undrained creep test for normally consolidated cohesive soils.
- (2) The anisotropic modified Cam-Clay model improved the model accuracy since it is fundamentally based on the normally consolidated clay.
- (3) The simplification of the generalized viscous theory was successful for the simulation of the creep behaviors adopted in this research.
- (4) The inclusion of a damage law made it possible for the model to satisfactorily simulate undrained creep rupture under different stress levels.
- (5) Despite the simplicity of the constitutive model, it performs well as long as the time to failure ratio of the creep rupture tests is within the same order of magnitude. Otherwise, it becomes necessary to use

different damage parameter values for different tests.

## References

1. Al-Sharmani, M. A. and Sture, S. (1994), "Characterization of Time dependent Behavior of Anisotropic Cohesive Soils", *Computer Methods and Advances in Geomechanics*, Siriwardane and Zaman (eds.) pp.505-511.
2. Aubry, D., Kodaissi, E. and Meimon, E., A. (1985), "Viscoplastic Constitutive Equations for Clays including Damage Law", *Proc. 5th Int. Conf. Numerical Methods in Geomechanics*, Vol.1, pp. 421-428.
3. Bonaparte, R. (1981), *A Time-dependent Constitutive Model for Cohesive Soils*, Ph. D. Dissertation, Univ. of California at Berkeley
4. Borja, R. I. (1984), *Finite Element Analysis of the Time-dependent Behavior of Soft Clays*, Ph. D. Dissertation, Stanford Univ.
5. Chiarelli, A. S., Shao, J. F., and Hoteit, N. (2003), "Modeling of Elastoplastic Damage Behavior of a Claystone", *Int. J. of Plasticity*, Month. 1, pp.23-45.
6. Dafalias, Y. G. (1982), "Bounding Surface Elastoplasticity-Viscoplasticity for Particulate Cohesive Media", *Proc. IUTAM Symposium on Deformation and Failure of Granular Materials*, P. A. Vermeer and H. J. Luger (eds.), A. A. Balkema, Publishers, Rotterdam, pp.97-107
7. Dafalias, Y. F. (1987), *An Anisotropic Critical State Clay Plasticity Model. Constitutive Laws for Engineering Materials: Theory and Applications*, Elsevier Science Publishing Co. Inc., pp. 513-521.
8. de Sciarra F. M. (1997), "General Theory of Damage Elastoplastic Models", *J. of Engineering Mechanics*, Vol.123, No.10, pp. 1003-1011.
9. Jenson, R. P., Plesha M. E., Edil, T. B., Bosscher P. J., and Kahla, N. B. (2001), "DEM Simulation of Particle Damage in Granular Media", *Int. J. of Geomechanics*, pp.21-39
10. Kachanov, L. M. (1967), *The Theory of Creep : Part I*, National Lending Library for Science and Technology, Boston
11. Matsui, T. and Abe, N.(1988), "Verification of Elasto-viscoplastic Model of Normally Consolidated Clays in Undrained Creep", *Pro. 6th Int. Conf. of Numerical Methods in Geomechanics*, Vol.1, pp. 453-459.
12. Murayama, S., Kurihara, N. and Sekiguch, H. (1970), *On Creep Rupture of Normally Consolidated Clays*, Annuals, Disaster Prevention Research Institute, Kyoto University, No. 13B, pp. 525-541
13. Perzyna, P. (1966), "Fundamental Problems in Viscoplasticity", *Advances in Applied Mechanics*, Vol.9, pp.243-377
14. Regel, V. R., Slutsker, A. I. and Tomashevsky, E. K. (1974), *Kinetics Nature of Strength in Solid Bodies*, Nauka, Moscow
15. Sekiguchi, H. (1984), "Theory of Undrained Creep Rupture of Normally Consolidated Clay Based on Elasto-Viscoplasticity", *Soils and Foundations*, Vol.24, No.1, pp.129-147
16. Singh, A. and Mitchell, J. K. (1968), "General Stress-Strain-Time Function for Soils", *J. of Soil Mechanics and Foundation*, Vol. 94, No.SM1, pp.21-46
17. Vaid, Y. P. and Campanella, R. G. (1977), "Time-dependent Behavior of Undrained Clay", *J. of Geotechnical Engineering*, No. GT 7, pp.693-709.
18. Vyalov, S. S. (1986), *Rheological Fundamentals of Soil Mechanics*, Elsevier Science Publishing Company Inc., New York.

(received on May 20, 2004, accepted on Sep. 18, 2004)